SPANWISE DISTRIBUTION OF VORTEX DRAG AND LEADING-EDGE SUCTION IN SUBSONIC FLOW

Professor Dr.-Ing. Siegfried N. Wagner
Institut für Luftfahrttechnik und Leichtbau
Hochschule der Bundeswehr München
D-8014 Neubiberg, F.R.G.

Abstract

Using the author's lifting surface theory and investigations by Carlson and Mack on two-dimensional airfoil sections, spanwise distribution of the induced drag or vortex drag of swept and delta wings is calculated as a function of lift at subsonic speeds. The influences of Mach number, Reynolds number and wing parameters, e.g. local thickness to chord ratio, location of maximum wing section thickness as fraction of chord, local leading-edge radius and leading-edge sweep are taken into account. The discrepancies of induced drag between potential flow calculation and experiment can be reduced by the new method. The applicability of the method is demonstrated by comparison between calculations and experiments of the spanwise distribution of leading-edge thrust and of induced drag.

I. Introduction

The objective of the present study is to calculate the spanwise distribution of the leading-edge-suction force of wings with arbitrary planforms on the basis of linear, subsonic thin wing theory (the author's lifting-surface theory[1]) and of investigations by Carlson and Mack[2] on two-dimensional profile sections which contain the influence of Mach number, Reynolds number and geometric parameters like thickness ratio, position of maximum thickness, and leading-edge radius.

An accurate method for calculating the suction-force distribution of wings is important for the following, purely academic reasons:

1. The spanwise distribution of thrust which is the streamwise component of suction force is necessary to accurately compute the spanwise distribution of induced drag of swept wings.

2. The total thrust can be obtained either by integrating the thrust distribution or by using the thrust component of the total lift force and of the total induced drag which can be calculated by Munk's theory[3]. The comparison of the total thrust computed by these two different methods is a very sensitive indicator of the numerical accuracy of a lifting-surface theory since the thrust distribution depends on the distribution of the spanwise loading to the second power. The possibility of such an accuracy check was previously noted by H. Multhopp[4].

The suction force stems from the low pressures induced by the high velocities around the leading edge of wings at subsonic speeds. It also occurs at supersonic speeds, if there is a subsonic leading edge. The development of suction force is of interest because it counteracts the drag and permits high aerodynamic efficiency of wings at lifting conditions. However, the theoretically predicted full suction force is very seldom achieved in real flow. Therefore, the prediction of real suction plays an important role in aircraft design for the following reasons:

1. The calculation of suction force distribution in real flow and thus the prediction of realistic lift-dependent drag is necessary for a reliable optimization of the wing design point, for a reliable prediction of range and for a reliable estimate of the productivity of an airplane.

2. A knowledge of the spanwise leading-edge thrust distribution improves the designer's ability to prevent flow separation at the leading edge, since the regions of high leading-edge-suction force are also the areas where leading-edge flow separation would most likely occur.

3. Thin low-aspect ratio wings have significant nonlinear lift and pitching moment due to vortex flow near the wing-leading edge. The difference between the theoretically predicted and the actual suction force can be used as a basis to compute nonlinear lift and pitching moment according to the Polhamus[5] concept.

The findings and the accuracy of the present method are demonstrated by calculating the loading, spanwise thrust, and vortex-drag distribution of several wings. The results are compared with experiments.

II. Integral Equation of Lifting-Surface Theory for Calculating the Pressure Distribution of Wings

Lifting-surface theory[1] leads to the following singular integral equation for the unknown pressure distribution, Δc_p:

$$\alpha_F - \frac{\partial z(\xi,\eta)}{\partial x} = -\frac{1}{8\pi} \oint_{-1}^{+1} \int_{\xi_{le}}^{\xi_{te}} \frac{\Delta c_p(\xi',\eta')}{(\eta-\eta')^2} \times \left\{ 1 + \frac{\xi - \xi'}{\left[(\xi-\xi')^2 + \beta^2(\eta-\eta'^2)\right]^{1/2}} \right\} d\xi' d\eta' \qquad (1)$$

This integral contains a strong singularity at $\eta \rightarrow \eta'$ and has to be defined by

$$\oint_{-1}^{+1} \frac{g(\xi,\eta,\eta')}{(\eta-\eta')^2}\, d\eta' = \lim_{\varepsilon \rightarrow 0} \left[\int_{-1}^{\eta-\varepsilon} \frac{g(\xi,\eta,\eta')}{(\eta-\eta')^2}\, d\eta' + \int_{\eta+\varepsilon}^{+1} \frac{g(\xi,\eta,\eta')}{(\eta-\eta')^2}\, d\eta' - \frac{2}{\varepsilon}\, g(\xi,\eta,\eta) \right]$$

$$\xi_{le} < \xi \leqq \xi_{te} \quad . \tag{2}$$

The wing geometry, the coordinate system used, and the angle-of-attack distribution, $\alpha_F - \partial z/\partial x$ are defined in Fig. 1. If uncambered profiles are used, then $\alpha_o = 0$ and $\partial z/\partial x = -\Theta(\eta)$; the left side of eq. (1) then contains only the geometric angle of attack, $\alpha_g(\eta) = \alpha_F + \Theta(\eta)$. If, in addition, the wing has no twist, i.e., if $\Theta(\eta) = 0$, the left side of eq. (1) consists only of the angle α_F = const.

The pressure distribution is represented by a linear combination of spanwise and chordwide pressure distribution functions (pressure modes):

$$\Delta c_p = \frac{2b}{c(\eta)} \sum_{n=0}^{N} h_n(\xi) \cdot f_n(\eta) \quad . \tag{3}$$

Thus, the integration of eq. (1) in chordwise direction can be separated from the integration in spanwise direction:

$$\alpha_F - \frac{\partial z}{\partial x}(\xi,\eta) = -\frac{1}{2\pi} \sum_{n=0}^{N} \oint_{-1}^{+1} \frac{H_n(\xi,\eta,\eta')}{(\eta-\eta')^2}\, f_n(\eta')\, d\eta' \quad , \tag{4a}$$

$$H_n(\xi,\eta,\eta') = H_n(X,Y) = \int_0^1 h_n(X') \left\{ 1 + \frac{X-X'}{\left[(X-X')^2 + Y^2\right]^{1/2}} \right\} dX' \tag{4b}$$

where

$$X = [b/2c(\eta')]\,[\xi - \xi_{le}(\eta')]\,,$$

$$X' = [b/2c(\eta')]\,[\xi' - \xi_{le}(\eta')]\,,$$

$$Y = [b\beta/2c(\eta')]\,(\eta-\eta') \quad . \tag{5}$$

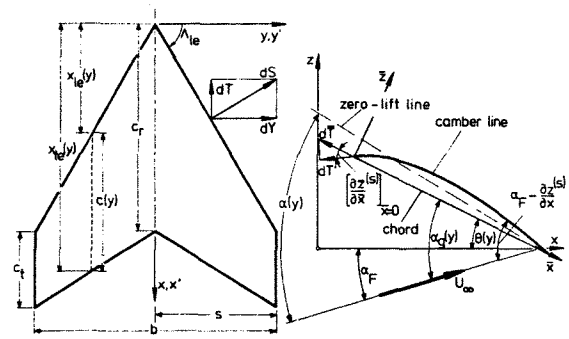

Fig. 1: Coordinate System

Following the basic assumptions of Multhopp[4] and Truckenbrodt[6], the chordwise pressure modes $h_n(\xi)$ are prescribed by utilizing the pressure distribution functions of two-dimensional thin-airfoil theory (the arguments justifying this assumption are discussed in Ref. 7):

$$h_n(X) = \frac{1}{\pi} \sqrt{\frac{1-X}{X}} \left[\frac{T_n(1-2X) + T_{n+1}(1-2X)}{1 - X} \right],$$

$$n = 0,1,2,\ldots,N \quad . \tag{6}$$

The functions T_n are Chebyshev polynomials of the first kind with the argument 1-2X. It has been shown that the spanwise pressure modes

$$c_n(\eta) = [2b/c(\eta)]\; f_n(\eta) \tag{7}$$

have a physical meaning when the pressure distribution functions $h_n(\xi)$ of eq. (6) are used. For instance, c_o and c_1 are proportional to the local lift and local pitching moment, respectively:

$$c_o(\eta) = c_l(\eta) \quad \text{and} \quad c_1(\eta) = 4c_m(\eta) \quad . \tag{8}$$

Since the chordwise pressure modes are prescribed, the integration in chordwise direction is reduced to the evaluation of the so-called influence functions $H_n(X,Y)$ in eq. (4b), which now depend only on the geometry of the wing planform and the Mach number. Thus, the integral equation for the unknown pressure distribution $\Delta C_p(\xi,\eta)$ given in eq. (1) is transformed into a system of integral equations for the unknown spanwise pressure modes $f_n(\eta)$, eq. (4a). The solution of that system of integral equations is explained in Ref. 1. The unknown functions are expressed as trigonometric interpolation polynomials

$$f_n(\Theta) = \sum_{m=1}^{M} f_{nm}\, s_m(\Theta) \tag{9a}$$

where

$$s_m(\Theta) = \frac{2}{M+1} \sum_{\mu=1}^{M} \sin\mu\Theta_m \sin\mu\Theta \quad , \qquad (9b)$$

and

$$\Theta = \arccos\eta \quad . \qquad (9c)$$

The integration stations are defined in such a manner that the function values themselves, $f_{nm} = f_n(\Theta_m)$, instead of the Fourier coefficients, appear as the unknowns. This amounts in fact to a linear transformation of the integral equation. The functions f_{nm} are the values of the spanwise pressure modes $f_n(\eta)$ at locations

$$\eta_m = \cos\Theta_m, \quad \Theta_m = \pi m/(M+1), \quad m = 1,2,\ldots,M \quad .$$

III. Calculation of Spanwise Distribution of Induced Drag and Leading-Edge-Suction Force

In order to calculate the spanwise distribution of induced drag of swept wings, one has to compute the spanwise distribution of lift and thrust, which is the component of suction force in streamwise direction. The spanwise distribution of thrust has been derived in Ref. 1 for planar wings. It can be shown that the formula for the non-dimensional thrust distribution (1)

$$\tau(\eta) = \frac{c_t(\eta)\cdot c(\eta)}{2b} =$$

$$= \frac{b(1+\beta^2\cot^2\Lambda_{le})^{1/2}}{\pi c(\eta)\cdot\cot\Lambda_{le}} \left[\sum_{n=0}^{N} f_n(\eta)\right]^2 \qquad (10)$$

is also valid for wings of low camber. The local thrust, $d\bar{T}$ and the local normal force, $d\bar{N}$, act in the direction of the local chord ($\bar{x}$ axis) and normal to it ($\bar{z}$ axis), respectively. In the case of a twisted wing, the coefficient of total thrust is calculated in the x,y plane:

$$C_T = A \int_{-1}^{+1} \frac{\tau(\eta)\cos\alpha_F - \gamma(\eta)\sin\varepsilon}{\cos(\alpha_F+\varepsilon)} d\eta \quad . \qquad (11)$$

The coefficient of the total induced drag can now be obtained by integrating the thrust distribution:

$$C_{D_i} = A \int_{-1}^{+1} \left[\gamma(\eta)\tan(\alpha_F+\varepsilon) - \frac{\tau(\eta)}{\cos(\alpha_F+\varepsilon)}\right] d\eta \quad . \qquad (12)$$

The coefficient of total lift is:

$$C_L = A \int_{-1}^{+1} f_0(\eta)d\eta = A \int_{-1}^{+1} \gamma(\eta)d\eta =$$

$$= \frac{\pi A}{M+1} \sum_{m=1}^{M} \gamma(\Theta_m) \sin\Theta_m \quad . \qquad (13)$$

The relations derived so far are only valid within the limitations of linear, subsonic thin wing theory. This method provides an estimate of the theoretical thrust only which may or may not be attainable in the real flow. Fortunately, a recent paper of Carlson and Mack (2) describes an empirical method for the estimation of attainable thrust on the basis of theoretically predicted thrust. This method has been programmed as a subroutine in the existing lifting-surface computer program of the author (1). The set of equations for use in prediction of attainable thrust according to Ref.2 is summarized as follows:

The normal airfoil parameters (Fig.2) must be computed as a function of streamwise airfoil parameters for a series of spanwise wing stations. The normal flow Mach number is defined as

$$M_n = M_\infty \cos\Lambda_{le} \quad . \qquad (14)$$

The ratio of the normal section chord to the streamwise section chord is obtained from

$$\frac{c_n}{c} = \frac{2\xi_D}{\sin\Lambda_{le}[(1-\xi_D)\tan\Lambda_{le}+\xi_D\tan\Lambda_{te}]+\cos\Lambda_{le}} \qquad (15)$$

The thickness-to-chord ratio of the normal section is

$$\delta_n = \frac{d_n}{c_n} = \frac{d}{c}\frac{1}{2\xi_D\cos\Lambda_{le}} \qquad (16)$$

and the ratio of the leading-edge radius to chord for the normal section is expressed as

$$\frac{r_n}{c_n} = \frac{r}{c}\cdot\frac{1}{2\xi_D\cos^2\Lambda_{le}} \quad . \qquad (17)$$

The normal section thrust coefficient is related to the streamwise section thrust coefficient by

$$c_{t,n} = c_t \frac{c}{c_n}\frac{1}{\cos^2\Lambda_{le}} \quad . \qquad (18)$$

The normal flow Reynolds number is

$$R_n = R \frac{c_n}{c} \cos\Lambda_{le} \quad . \tag{19}$$

In addition, an effective limiting pressure coefficient is defined as a function of the local Mach number and Reynolds number normal to the leading edge:

$$c_{p,lim} = \frac{-2}{\gamma M_n^2} \times \left[\frac{R_n \cdot 10^{-6}}{R_n \cdot 10^{-6} + 10^{(4-3M_n)}} \right]^{0.05+0.35(1-M_n)^2} . \tag{20}$$

In contrast to that limiting pressure coefficient, the pressure coefficient of thin wing theory has a square root singularity at the leading edge. Thus, the pressure coefficient may have values that are far beyond vacuum and that can never be obtained in real flow.

Furthermore, an effective local Mach number is defined in Ref. 2:

$$M_e = \frac{-\sqrt{2}}{\kappa} \left[\sqrt{1+\kappa^2} - 1 \right]^{1/2} , \tag{21a}$$

where

$$\kappa = \gamma c_{p,lim} \sqrt{1-M_n^2} , \tag{21b}$$

where γ is the ratio of specific heats. Finally, the ratio of the attainable thrust, C_t^*, to the theoretical leading-edge thrust, C_t, is

$$K_t = c_t^*/c_t = \frac{2(1-M_e^2)}{M_e} \left[\frac{\delta_n (r_n/c_n)^{0.4}}{c_{t,n} \cdot \cos\delta_{le} \sqrt{1-M_n^2}} \right]^{0.6} , \tag{22}$$

but not greater than 1.0:

δ_{le} is the deflection angle of the leading edge of a cambered wing and is defined

$$\tan\delta_{le} = \lim_{\bar{x} \to 0} (\partial \bar{z}/\partial \bar{x}) \quad . \tag{23}$$

In the case of an uncambered wing, δ_{le} is equal to zero.

In regions of the wing leading edge away from the apex, away from the wing-body juncture, and away from the wing tip, the preceding expressions are believed to provide reasonable results on the basis of the empirical two-dimensional investigations of Carlson and Mack (8). Wing-body configurations can not be handled by the author's lifting surface program. Near the apex, thrust values of swept wings are generally small and errors in the attainable levels should have a small influence on the total thrust and induced drag. The influence of three-dimensional flow near the wing tip can only be investigated by comparison with experiments.

On the basis of C_t^*, the thrust coefficient in real flow, a nondimensional thrust distribution can be defined:

$$\tau^*(\eta) = \frac{c_t^*(\eta)\, c(\eta)}{2b} = K_t \cdot \tau(\eta) \quad . \tag{24}$$

The coefficient of total thrust is now:

$$C_T^* = A \int_{-1}^{+1} \frac{\tau^*(\eta)\cos\alpha_F - \gamma(\eta)\sin\varepsilon}{\cos(\alpha_F+\varepsilon)} d\eta \quad . \tag{25}$$

The coefficient of total induced drag in real flow can now be obtained by integrating the realistic thrust distribution:

$$C_{D_i}^* = A \int_{-1}^{+1} \left[\gamma(\eta)\tan(\alpha_F+\varepsilon) - \frac{\tau^*(\eta)}{\cos(\alpha_F+\varepsilon)} \right] d\eta . \tag{26}$$

If the suction force is equal to zero, the induced drag is calculated by

$$C_{D_i}/(C_L-C_{L_O})^2 = 1/(dC_L/d\alpha) \quad (C_T = 0) \quad . \tag{27}$$

This case describes the maximum induced drag in subsonic flow.

IV. Results

Since the prediction method of actual spanwise distribution of induced drag is based on two-dimensional flow considerations, it should yield fairly accurate results for wings where the flow has mainly almost two-dimensional character, e.g. high aspect-ratio wings with little leading-edge sweep. The question is how accurate the prediction will be if the wing has a

low aspect ratio and a large leading-edge sweep, as in case of a delta wing. Carlson and Mack[2] got good results when comparing the theoretical values of the total axial force coefficient and of the total drag coefficient with experiments. A more severe test of the method will be given in correlations with data of the spanwise distribution of leading-edge thrust and of the induced drag.

The spanwise distribution of the local leading-edge suction force of a thin plane delta wing was measured by Ridder[9],[10]. The planform of the wing has a leading-edge sweep angle of 60 degrees, the wing tip is cropped 10 per cent of the full triangular semispan giving an aspect ratio of 1.889. The wing was made from a thin plate of sheet metal and has a cylindrical thickness distribution with constant section normal to the leading edge. The thickness distribution does only cover the front of the local wing chord and is 26,5 per cent of the local chord at 55,56 per cent of semispan in case of the first period of experiments[9]. The airfoil section is elliptical and is faired with plane tangents to the flat plate rear end of the wing. The leading edge of the port wing panel is divided into 8 equal length elements to measure the local normal and tangential force [9]. According to Ridder [10], the experiences gained with the extremely delicate balance, with the associated sealing problems and "base" pressure correction in Ref. 9 led to a simpler and more robust method to measure the local suction force by means of the pressure from a single pressure tap at about 35 rectangular panels at the leading edge [10]. However, the latter method is restricted to low angles of attack for which attached leading edge flow is maintained.

In Fig. 3, the local thrust factors K_t versus span are shown for several angles of attack. Up to an angle of four degrees, K_t is equal to 1, i.e., there is full thrust. Ridder[10] made the same observation. At higher angles of attack, full thrust is no longer obtained as shown by the distribution of K_t. Towards the tip of the wing, K_t approaches 1 again and stems from the two-dimensional flow considerations of Ref. 2. In practice, however, K_t should at least not increase towards the tip. Therefore, there are dashed lines in Fig. 3, which indicate the three-dimensional character of the flow and which cannot be predicted properly by the present method.

Some comparisons of theory and experiment[9],[10] are shown in Figs. 4 and 5 for the delta wing of Ridder's experiments. Fig. 4 contains the spanwise distribution of thrust coefficient C_t at full thrust condition and the spanwise distribution of C_t^* which designates the attainable thrust condition. Up to an angle of attack of 4 degrees (Fig. 4a) the agreement between theory and experiment is excellent, except a very small region near the wing tip. In this case the attainable thrust C_t^* is equal to the full thrust C_t. Beginning with $\alpha = 5$ degrees (Fig. 4b), the attainable thrust deviates from the theoretical thrust with increasing angle of attack (Fig. 4c and d). The thrust break-down starts from the wing tip and progresses towards the apex with increasing angle of attack. The agreement between theory and experiment is very good at the inner portions of the wing, but becomes poor at the tip and at higher angles of attack. Here, the three-dimensional character of the flow and of the boundary layer cannot be predicted on the basis of this method.

Fig. 5 shows the overall lift dependent drag coefficient $C_D - C_{D_0}$ and the overall thrust coefficients C_T (full thrust) and C_T^* (attainable thrust) as functions of the total lift coefficient C_L. The limiting conditions of zero and full theoretical thrust are also shown in Fig. 5a. It is interesting to note that the agreement between theory and experiment is very good in the case of the total drag coefficient, whereas in the case of the spanwise distribution of the thrust coefficient the agreement was not as good (Fig.4). Obviously, the reason for this fact is some compensating errors when calculating the total drag coefficient according to

$$C_{D_i}^* = C_L - C_T^* \tag{28}$$

The predicted thrust is larger than the measured one. The theoretical lift coefficient is also larger than the actual one. These two errors are possibly compensated by eq. (28).

The comparisons of theory and experiment are shown in the following figures, beginning with Fig. 6, and are made for a double delta wing of a fighter aircraft model, the design of which is discussed in Ref. 11. The tests were made with an uncambered and untwisted wing No. I and with a twisted and cambered wing No. II. The wing has an aspect ratio of approximately 2.25 and a taper ratio of 0.1.

The lift is calculated in two different ways, namely using potential flow theory (linear lift) and using Polhamus' concept[5] (nonlinear lift). In the latter case, the difference between theoretical thrust and attainable thrust is rotated by 90 degrees and is regarded as the nonlinear part of lift.

Figs. 6-14 contain the results for the uncambered and untwisted wing I: Fig. 6a shows the comparison between theory and experiment for the lift for a Mach number

of 0.5. Although the influence of viscosity can not be treated by theory, the measured lift is higher at larger angles of attack than the linear lift. Using Polhamus' concept brings the nonlinear lift closer to the test data which show nonlinear lift because of a large leading-edge sweep angle of the inboard panel. The deviation of attainable thrust from theoretical, full thrust shows Fig. 6b.

Fig. 7a shows the lift-dependent drag factor $k = \pi\Lambda \cdot \partial C_W / \partial (C_L^2)$ as a function of C_L. This factor is very sensitive to the determination of drag. The theory is optimistic compared to measurement. In Fig. 7b $C_D - C_{D_O}$ is plotted versus C_L. At low C_L levels the agreement between theory and measurement is very good. At higher C_L levels the prediction of L/D would be too pessimistic using linear lift and is too optimistic in the case of computing nonlinear lift.

Fig. 8 compares the spanwise distribution of the theoretical thrust c_t and of attainable thrust c_t^* at a Mach number of 0.5 and for various angles of attack. Up to an angle of attack of 2 degrees (Fig.8a) full theoretical thrust is obtained. Beginning with an angle of attack of 3 degrees (Fig. 8b), the attainable thrust deviates from the theoretical thrust with increasing angle of attack (Figs. 8c and 8d). The thrust break-down starts from the wing tip and progresses towards the apex with increasing angle of attack.

Because of the break in leading-edge sweep of a double delta wing, thin wing theory predicts a jump of the spanwise distribution of thrust. This would never occur in nature. It is interesting to note that the present method removes almost completely that jump and approaches better reality.

Figs. 9 and 10 contain the results for the planar wing at a Mach number of 0.7.

The agreement between theory and measurement is similarly good as in the case of a Mach number of 0.5.

In Fig. 11 and 12 the results for the planar wing are shown for a Mach number of 0.9. Since the wing is very thin, the present method which is only applicable to subsonic flow shows still good agreement with measurement (Fig. 11). The thrust break-down starts already at an angle of attack of 2 degrees (Fig. 12b).

Figs. 13 and 14 contain the results of the planar wing at a Mach number of 0.95. The deviations between theory and test data become larger for the drag polar at higher values of C_L. Obviously compressibility effects at transonic speed begin to develop which can not be treated by the present simple method for subsonic flow. The break-down of leading-edge thrust starts at an angle of attack of 2 degrees and progresses rapidly from the tip towards the apex with increasing angle of attack.

Figs. 15 and 16 show the results for the cambered and twisted double delta wing II discussed in Ref. 11. It is interesting to note that theory and measurement of the drag polar (Fig. 15b) agree better than in the case of the uncambered and untwisted wing I of the same planform (Fig.7b). Obviously, camber and twist helped to prevent an early break-down of thrust. This effect can clearly be seen from Fig. 16. Even at higher angles of attack the inboard panel develops high levels of thrust, and in this portion of the wing the development of thrust is desired. It should be noted that a Mach number of 0.5 is still an off-design condition, since the wing has been optimized for a Mach number range between 0.9 and 0.95 (see Ref. 11).

V. Concluding Remarks

On the basis of the author's lifting surface theory[1] and of investigations by Carlson and Mack[2] on two-dimensional airfoil sections, the spanwise distribution of thrust (and thus of induced drag) of swept wings with low aspect ratio has been calculated as a function of lift, Mach number and Reynolds number. Compared with the original thin wing theory, the new method allows to take into account the important parameters for suction force computation, e.g. Reynolds number, leading-edge radius, local thickness to chord ratio, and location of maximum wing section thickness as fraction of chord. The comparisons of the present method with measurement showed mostly good agreement and are very encouraging for further investigations. Since the computation time is very low, the present method is preferably applicable to design studies when a large number of parameters has to be varied.

It is intended to extend the computer program for the calculation of nonlinear pitching moment as soon as enough empirical data are evaluated to predict the location of the vortex produced by a sharp leading edge strake.

VII. Acknowledgments

The author wishes to thank the MBB Company for making available the test data[12] of the fighter aircraft model. Special thanks are due to Mrs. Dipl.-Math.S. Rezanka, who wrote the computer program to calculate and plot the spanwise distribution of attainable thrust and of actual induced drag and who did all the computations.

VIII. References

1. Wagner, S.:
"On the Singularity Method of Subsonic Lifting-Surface Theory". Journal of Aircraft, Vol. 6, No. 6, pp. 549-558, Nov.-Dec. 1969

2. Carlson, H.W., and Mack, R.J.: "Studies of Leading-Edge Thrust Phenomena." Journal of Aircraft, Vol.17, No.12, pp.890-897, Dec.1980.

3. Munk, M.M.: "Isoperimetrische Aufgaben aus der Theorie des Fluges". Dissertation, University of Göttingen, 1919. Also: NACA Rep. No.121, 1921.

4. Multhopp, H.: "Methods for Calculating the Lift Distribution of Wings. (Subsonic Lifting-Surface Theory)". A.R.C. Rep. and Mem. No.2884 (1955).

5. Polhamus, E.C.: "A Concept of the Vortex Lift of Sharp-Edge Delta Wings Based on a Leading-Edge-Suction Analogy". NASA TN-D3767, 1966.

6. Truckenbrodt, E.: "Tragflächentheorie bei inkompressibler Strömung". Wissenschaftliche Gesellschaft für Luftfahrt (WGL), Jahrbuch 1953, pp.40-65.

7. Wagner, S.: "Beitrag zum Singularitätenverfahren der Tragflächentheorie bei inkompressibler Strömung". Dissertation, Technical University of Munich, Jan. 1967.

8. Carlson, H.W., Mack, R.J., and Barger, R.L.: "Estimation of Attainable Leading-Edge Thrust for Wings at Subsonic and Supersonic Speeds". NASA TP-1500, 1979.

9. Ridder, S.-O.: "On the Induced Drag of Thin Plane Delta Wings. An Experimental Study of the Spanwise Distribution of the Leading Edge Forces at Low Speeds". Royal Institute of Technology, Department of Aeronautical Engineering, Stockholm, Technical Note KTH AERO TN 57, May 1971.

10. Ridder,S.-O.: "Experimental Study of Induced Drag and Leading Edge Tangential Suction Force Spanwise Distribution of Thin Plane Delta Wings at Low Speeds Including the Effects of Fuselage Diameter". Royal Institute of Technology, Department of Aeronautical Engineering, Stockholm, Technical Note KTH AERO TN 58, June 1972.

11. Sacher, P., Kraus, W., and Kunz, R.: "Computational Aerodynamic Design Tools and Techniques Used at Fighter Development". AGARD Symposium on "The Use of Computers as a Design Tool". AGARD-CP-280, pp. 16-1 to 16-12, Neubiberg, Germany, September 1979.

12. Messerschmitt-Bölkow-Blohm GmbH: Unpublished Data of MBB Measurements on a Figher Aircraft Model. 1979.

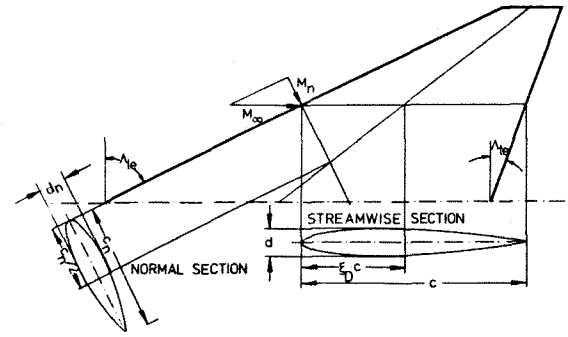

Fig.2 : Definition of normal airfoil sections for three - dimensional wings

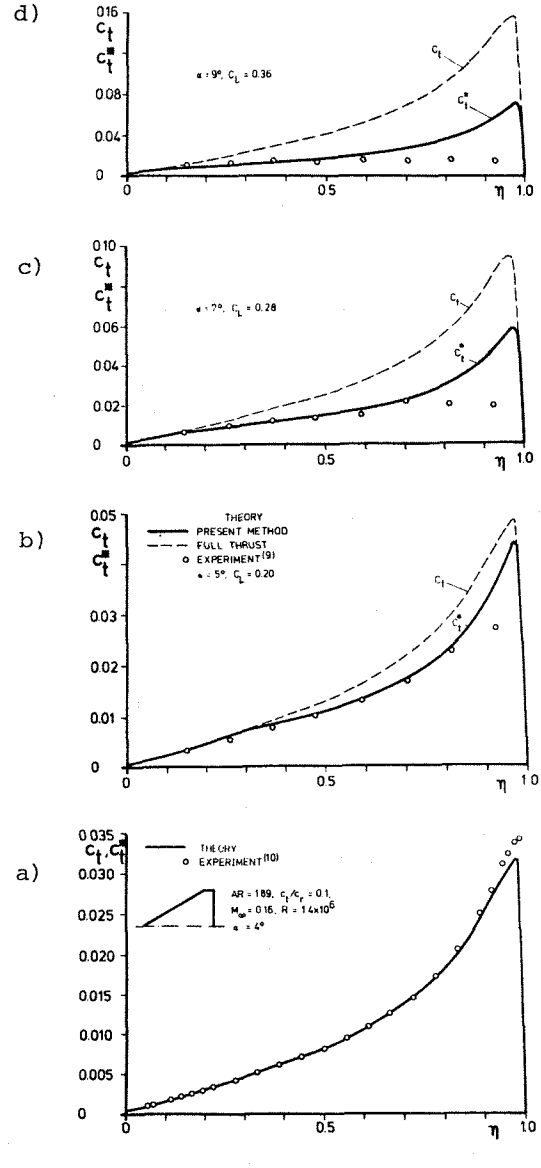

Fig.4 : Spanwise distribution of theoretical thrust c_t and attainable thrust c_t^* for a delta wing

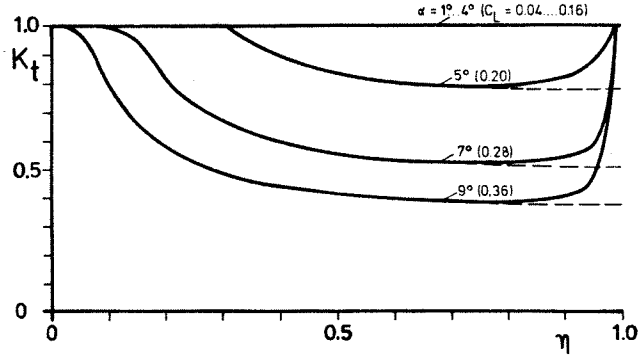

Fig.3 : Spanwise distribution of attainable thrust ratio or thrust factor K_t for a delta wing

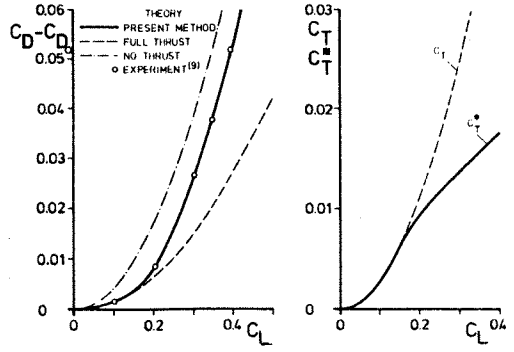

Fig.5 : Drag polar for a delta wing (computed and measured) and total theoretical and attainable thrust coefficient

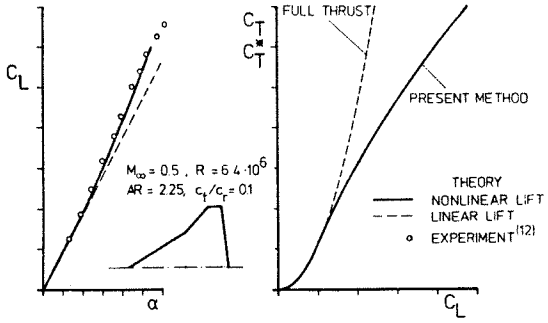

Fig.6 : Lift coefficient C_L as a function of angle of attack and thrust coefficient C_T versus C_L for a plane double delta wing at a Mach number of 0.5

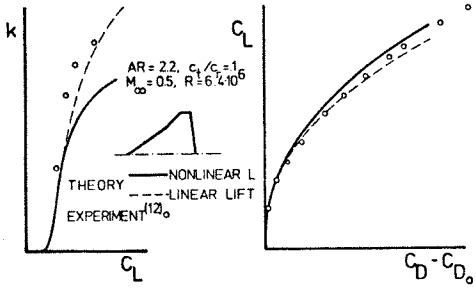

Fig.7 : Induced drag factor k and induced drag coefficient $C_D - C_{D_o}$ as a function of lift coefficient for a plane double delta wing at a Mach number of 0.5

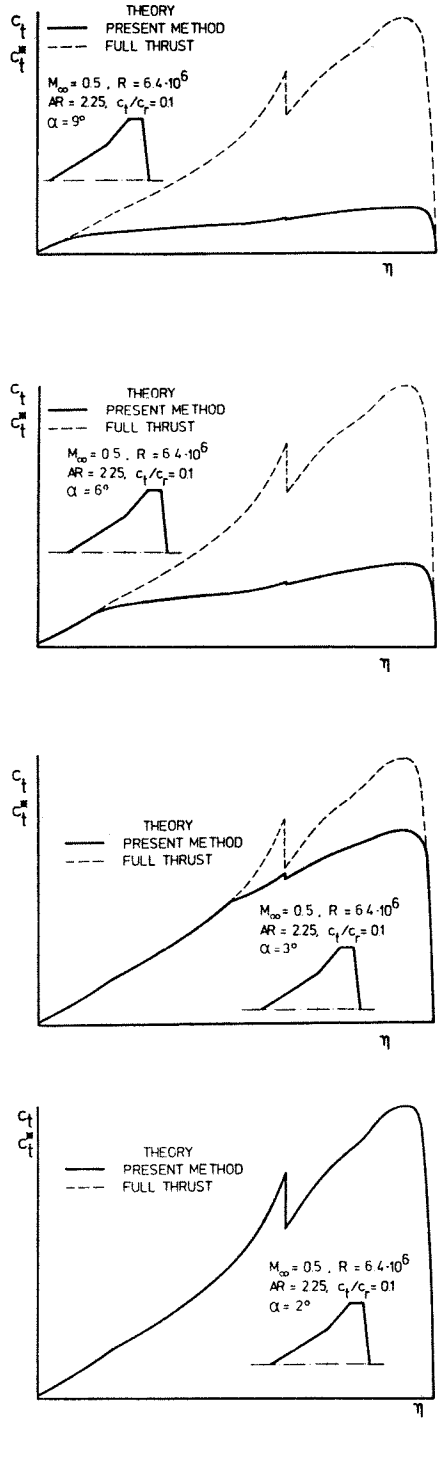

Fig.8 : Spanwise distribution of theoretical thrust c_t and attainable thrust c_t^* for a plane double delta wing at a Mach number of 0.5

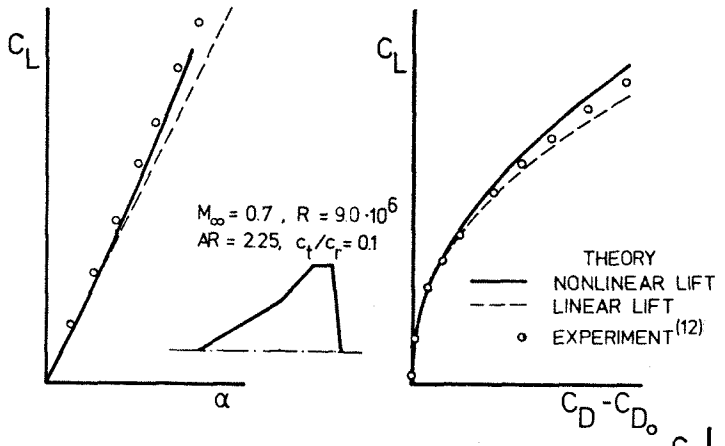

Fig.9 : Lift coefficient C_L versus angle of attack and induced drag $C_D - C_{D_o}$ versus C_L for a plane double delta wing at a Mach number of 0.7

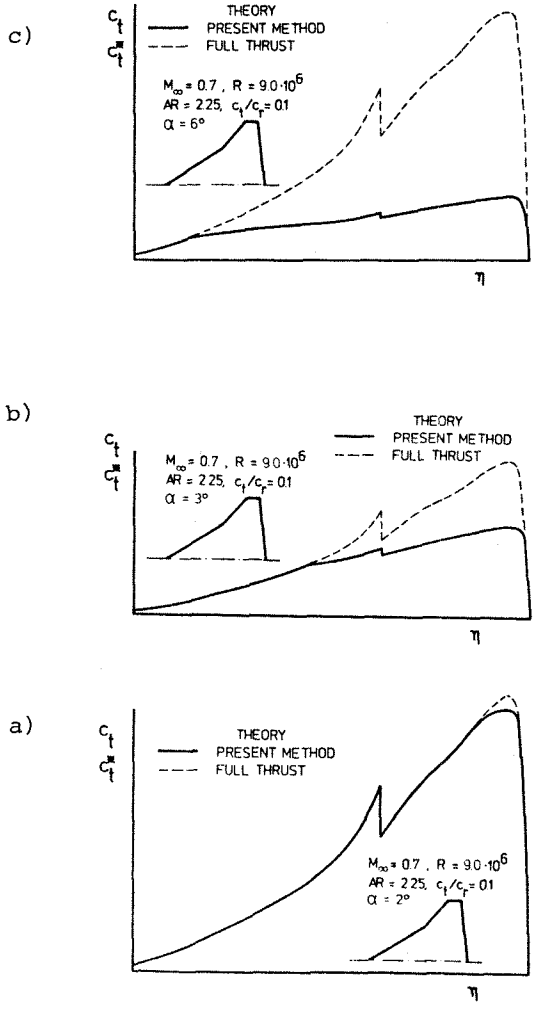

Fig.10: Spanwise distribution of theoretical thrust c_t and attainable thrust c_t^* for a plane double delta wing at a Mach number of 0.7

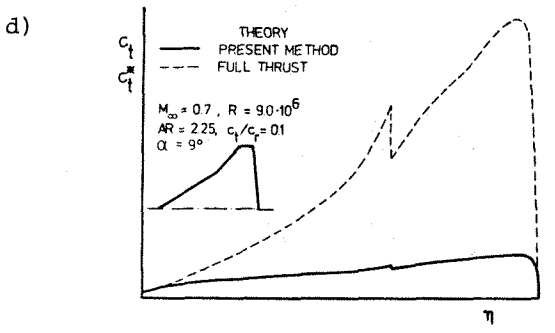

Fig. 10 (Cont.)

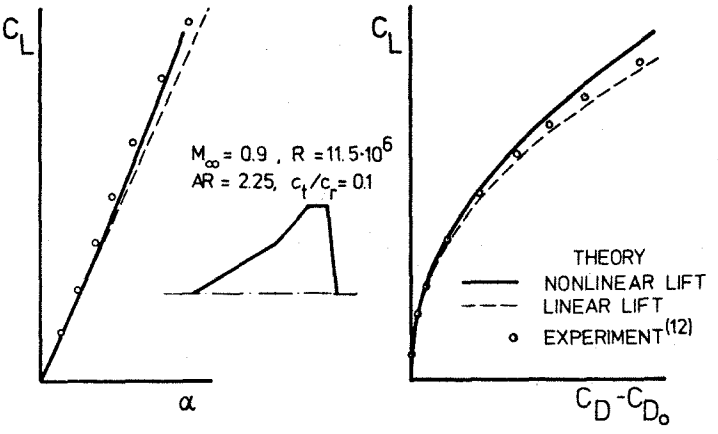

Fig.11: Lift coefficient C_L versus angle of attack and induced drag $C_D - C_{D_o}$ versus C_L for a plane double delta wing at a Mach number of 0.9

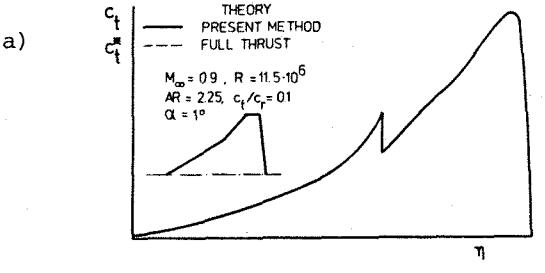

Fig.12: Spanwise distribution of theoretical thrust c_t and attainable thrust c_t^* for a plane double delta wing at a Mach number of 0.9

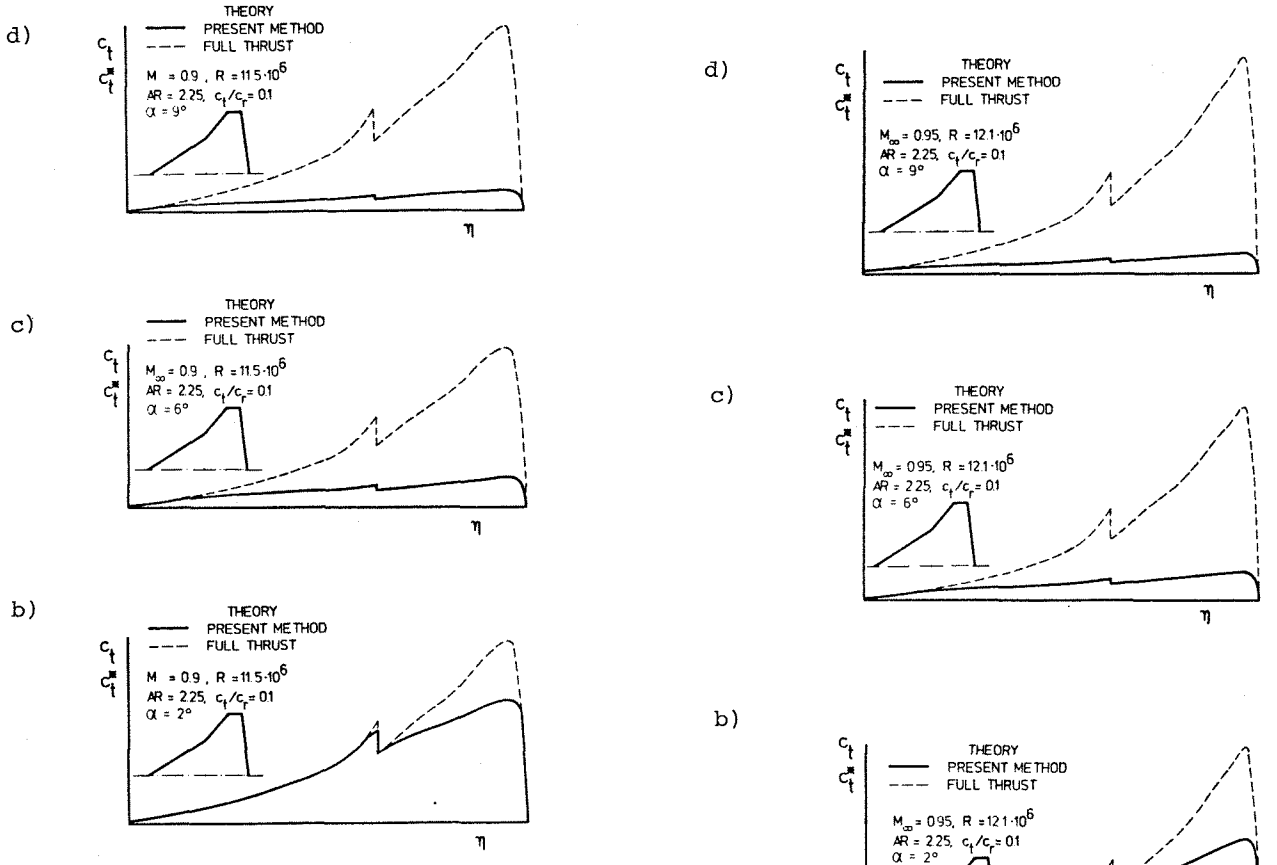

Fig. 12 (Cont.)

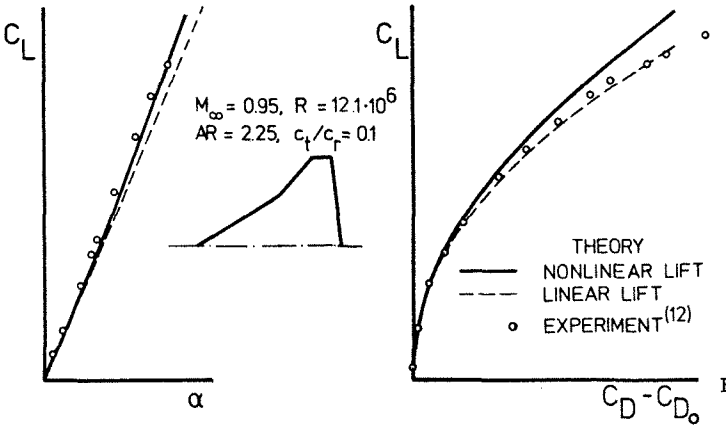

Fig.13: Lift coefficient C_L versus angle of attack and induced drag $C_D - C_{D_o}$ versus C_L for a plane double delta wing at a Mach number of 0.95

Fig.14: Spanwise distribution of theoretical thrust c_t and attainable thrust c_t^* for a plane double delta wing at a Mach number of 0.95

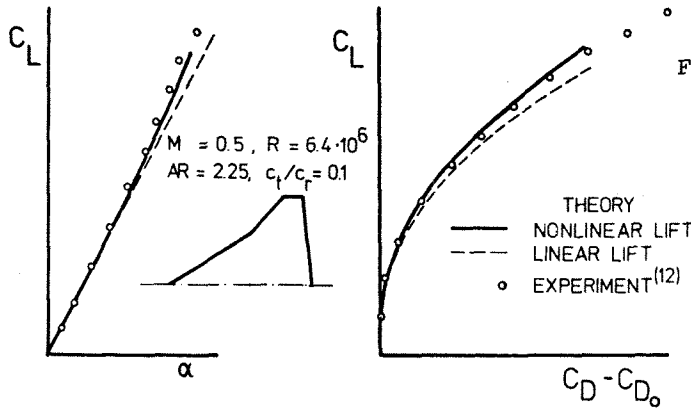

Fig.15: Lift coefficient C_L versus angle of attack and induced drag $C_D - C_{D_o}$ versus C_L for a cambered and twisted double delta wing at a Mach number of 0.5

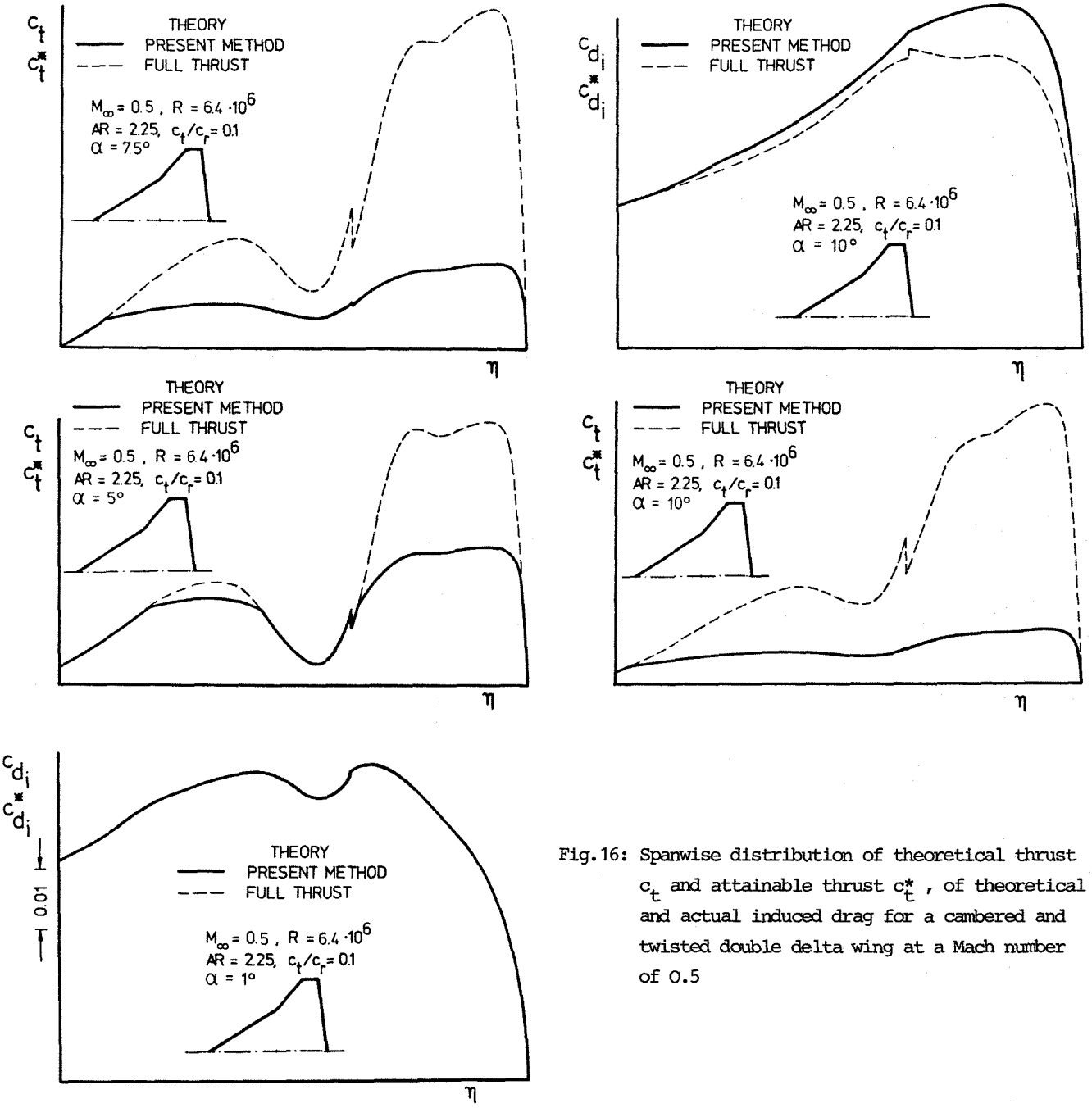

Fig.16: Spanwise distribution of theoretical thrust c_t and attainable thrust c_t^* , of theoretical and actual induced drag for a cambered and twisted double delta wing at a Mach number of 0.5